

Computer Simulation of Steady State Emission and Absorption Spectra for Molecular Ring

Pavel Heřman*, David Zapletal† and Milan Horák‡

*Department of Physics, Faculty of Science
University of Hradec Králové, Hradec Králové, Czech Republic
Email: pavel.herman@uhk.cz

†Institute of Mathematics, Faculty of Economics and Administration
University of Pardubice, Pardubice, Czech Republic
Email: david.zapletal@upce.cz

‡Faculty of Education
University of Hradec Králové, Hradec Králové, Czech Republic
Email: milan.horak@uhk.cz

Abstract—Knowledge of optical properties could shed more light on initial ultrafast phases of bacterial photosynthesis. Software package *Mathematica* is used for computer simulation of absorption spectra and steady state fluorescence spectra of ring molecular system, which can model cyclic antenna unit LH2 of the bacterial photosystem from purple bacterium *Rhodospseudomonas acidophila*. Three different models of uncorrelated static disorder are included in our simulations: Gaussian disorder in local excitation energies, Gaussian disorder in nearest neighbour transfer integrals and Gaussian disorder in radial positions of molecules in the ring. Dynamic disorder, interaction with a bath, is also included in Markovian approximation. The cumulant-expansion method of Mukamel et al. is used for the calculation of spectral responses of the system with exciton-phonon coupling. Calculated fluorescence spectra are compared with measured one. Values of the interpigment interaction energy and unperturbed transition energy from the ground state for above mentioned static disorder types are given.

Keywords—LH2 ring; exciton; fluorescence spectrum; static disorder; dynamic disorder; *Mathematica*.

I. INTRODUCTION

Ultrafast initial phases of photosynthesis in purple bacteria have been thoroughly studied over the last years. The bacterial light-harvesting complexes contain pigments circularly arranged in a protein scaffold. The crystal structure of peripheral light-harvesting complex LH2 from *Rhodospseudomonas acidophila* has been determined with high resolution [1], [2]. LH2 is a highly symmetric ring of nine pigment-protein subunits, each containing two transmembrane polypeptide helices and three bacteriochlorophylls (BChl).

In what follows, we are dealing with ring-shaped unit with nonameric symmetry resembling LH2 ring from *Rhodospseudomonas acidophila* with a strong interaction J between BChl molecules. Therefore, in our theoretical approach, an extended Frenkel exciton states model is considered. In spite of extensive investigation, the role of the protein moiety in

governing the dynamics of the excited states has not been totally clear yet. At room temperature, the solvent and protein environment fluctuate with characteristic time scales ranging from femtoseconds to nanoseconds. The simplest approach is to substitute fast fluctuations by dynamic disorder and slow fluctuations by static disorder.

In several steps, we have extended the former investigations of static disorder effect on the anisotropy of fluorescence made by Kumble and Hochstrasser [3] and Nagarajan et al. [4]–[6] for LH2 rings. After studying the influence of dynamic disorder for simple systems (dimer, trimer) [7]–[9] we added the dynamic disorder effect to our model of LH2 ring by using a quantum master equation in Markovian [10] and non-Markovian limits [11]. We also studied influence of four types of uncorrelated static disorder [12], [13] (Gaussian disorder in local excitation energies, transfer integrals, radial positions of BChls and angular positions of BChls on the ring) and influence of correlated static disorder (elliptical deformation) [11]. Models of rings with different arrangement of optical dipole moments (radial arrangement) were also investigated [14]–[16].

Recently, we have focused on the modeling of the steady state fluorescence spectra for molecular rings with 18 molecules and tangentially arranged optical transition dipole moments [17]. Main goal of the present paper is the investigation of absorption and steady state fluorescence spectra for different types of uncorrelated static disorder. The results for above mentioned three types of uncorrelated static disorder are compared with experimental fluorescence profile [18]. The dynamic disorder - interaction with the phonon bath in Markovian approximation for low and room temperature is taken into account simultaneously.

The remainder of this article is organized as follows. In Section II, we give the model of LH2 ring and review the theory we have used. In Section III, we mention computational point of view and used software. In Section

IV, we give the results of our absorption and steady state fluorescence spectra simulations, and in Section V, we draw some conclusions.

II. PHYSICAL MODEL

The Hamiltonian of an exciton in the ideal ring coupled to a bath of harmonic oscillators reads

$$H^0 = H_{\text{ex}}^0 + H_{\text{ph}} + H_{\text{ex-ph}}. \quad (1)$$

Here

$$H_{\text{ex}}^0 = \sum_{m,n(m \neq n)} J_{mn} a_m^\dagger a_n \quad (2)$$

corresponds to an exciton, e.g., the system without any disorder. The operator a_m^\dagger (a_m) creates (annihilates) an exciton at site m , J_{mn} (for $m \neq n$) is the so-called transfer integral between sites m and n .

The second term in (1),

$$H_{\text{ph}} = \sum_q \hbar \omega_q b_q^\dagger b_q, \quad (3)$$

represents phonon bath in the harmonic approximation (the phonon creation and annihilation operators are denoted by b_q^\dagger and b_{-q} , respectively).

Last term in (1),

$$H_{\text{ex-ph}} = \frac{1}{\sqrt{N}} \sum_m \sum_q G_q^m \hbar \omega_q a_m^\dagger a_m (b_q^\dagger + b_{-q}), \quad (4)$$

describes exciton-phonon interaction, which is assumed to be site-diagonal and linear in the bath coordinates (the term G_q^m denotes the exciton-phonon coupling constant).

Inside one ring, the pure exciton Hamiltonian can be diagonalized using the wave vector representation with corresponding delocalized "Bloch" states α and energies E_α . Considering homogeneous case with only nearest neighbour transfer matrix elements

$$J_{mn} = J_0 (\delta_{m,n+1} + \delta_{m,n-1}) \quad (5)$$

and using Fourier transformed excitonic operators (Bloch representation)

$$a_\alpha = \sum_n e^{i\alpha kn}, \quad \alpha = (2\pi/N)l, \quad l = 0, \pm 1, \dots, \pm N/2, \quad (6)$$

the simplest exciton Hamiltonian in α - representation reads

$$H_{\text{ex}}^0 = \sum_\alpha E_\alpha a_\alpha^\dagger a_\alpha, \quad E_\alpha = -2J_0 \cos \alpha. \quad (7)$$

Influence of uncorrelated static disorder is modeled by:

- (I) the local excitation energy fluctuations $\delta\varepsilon_n$ (uncorrelated, Gaussian distribution, standard deviation Δ , $H_s^I = \sum_n \delta\varepsilon_n a_n^\dagger a_n$),
- (II) the transfer integral fluctuations δJ_{mn} (uncorrelated, nearest neighbour approximation, Gaussian distribution, standard deviation Δ_J , $H_s^{II} = \sum_{mn(m \neq n)} \delta J_{mn} a_m^\dagger a_n$),

- (III) fluctuations of the radial positions of molecules on the ring δr_n (uncorrelated, nearest neighbour approximation, Gaussian distribution, standard deviation Δ_r).

Hamiltonian of the uncorrelated static disorder H_s^x adds to the Hamiltonian of the ideal ring H_{ex}^0 .

The cumulant-expansion method of Mukamel et al. [19], [20] is used for the calculation of spectral responses of the system with exciton-phonon coupling. Absorption $OD(\omega)$ and steady-state fluorescence $FL(\omega)$ spectra can be expressed as

$$OD(\omega) = \omega \sum_\alpha d_\alpha^2 \times \times \text{Re} \int_0^\infty dt e^{i(\omega - \omega_\alpha)t - g_{\alpha\alpha\alpha\alpha}(t) - R_{\alpha\alpha\alpha\alpha}t}, \quad (8)$$

$$FL(\omega) = \omega \sum_\alpha P_\alpha d_\alpha^2 \times \times \text{Re} \int_0^\infty dt e^{i(\omega - \omega_\alpha)t + i\lambda_{\alpha\alpha\alpha\alpha}t - g_{\alpha\alpha\alpha\alpha}^*(t) - R_{\alpha\alpha\alpha\alpha}t}. \quad (9)$$

Here $\vec{d}_\alpha = \sum_n c_n^\alpha \vec{d}_n$ is the dipole strength of eigenstate α , c_n^α are the expansion coefficients of the eigenstate α in site representation and P_α is steady state population of the eigenstate α . The inverse lifetime of exciton state $R_{\alpha\alpha\alpha\alpha}$ [18] is given by the elements of Redfield tensor [21] (a sum of the relaxation rates between exciton states)

$$R_{\alpha\alpha\alpha\alpha} = - \sum_{\beta \neq \alpha} R_{\beta\beta\alpha\alpha}. \quad (10)$$

The g-function and λ -values in (8) and (9) are given by

$$g_{\alpha\beta\gamma\delta} = - \int_{-\infty}^\infty \frac{d\omega}{2\pi\omega^2} C_{\alpha\beta\gamma\delta}(\omega) \times \times \left[\coth \frac{\omega}{2k_B T} (\cos \omega t - 1) - i(\sin \omega t - \omega t) \right], \quad (11)$$

$$\begin{aligned} \lambda_{\alpha\beta\gamma\delta} &= - \lim_{t \rightarrow \infty} \frac{d}{dt} \text{Im} \{ g_{\alpha\beta\gamma\delta}(t) \} = \\ &= \int_{-\infty}^\infty \frac{d\omega}{2\pi\omega} C_{\alpha\beta\gamma\delta}(\omega). \end{aligned} \quad (12)$$

The matrix of the spectral densities $C_{\alpha\beta\gamma\delta}(\omega)$ in the eigenstate (exciton) representation reflects one-exciton states coupling to the manifold of nuclear modes. In what follows only diagonal exciton phonon interaction in site representation is used (see (4)), i.e., only fluctuations of pigment site energies are assumed and the restriction to completely uncorrelated dynamic disorder is applied. In such case each site (i.e., each chromophore) has its own bath completely uncoupled from the baths of the other sites. Furthermore it is assumed that these baths have identical properties [12], [22], [23]

$$C_{mm'n'}(\omega) = \delta_{mn} \delta_{mm'} \delta_{nn'} C(\omega). \quad (13)$$

After transformation to exciton representation we have

$$C_{\alpha\beta\gamma\delta}(\omega) = \sum_n c_n^\alpha c_n^\beta c_n^\gamma c_n^\delta C(\omega). \quad (14)$$

Several models of spectral density of the bath are used in literature [18], [24], [25]. In our present investigation we

have used the model of Kühn and May [24]

$$C(\omega) = \Theta(\omega) j_0 \frac{\omega^2}{2\omega_c^3} e^{-\omega/\omega_c} \quad (15)$$

which has its maximum at $2\omega_c$.

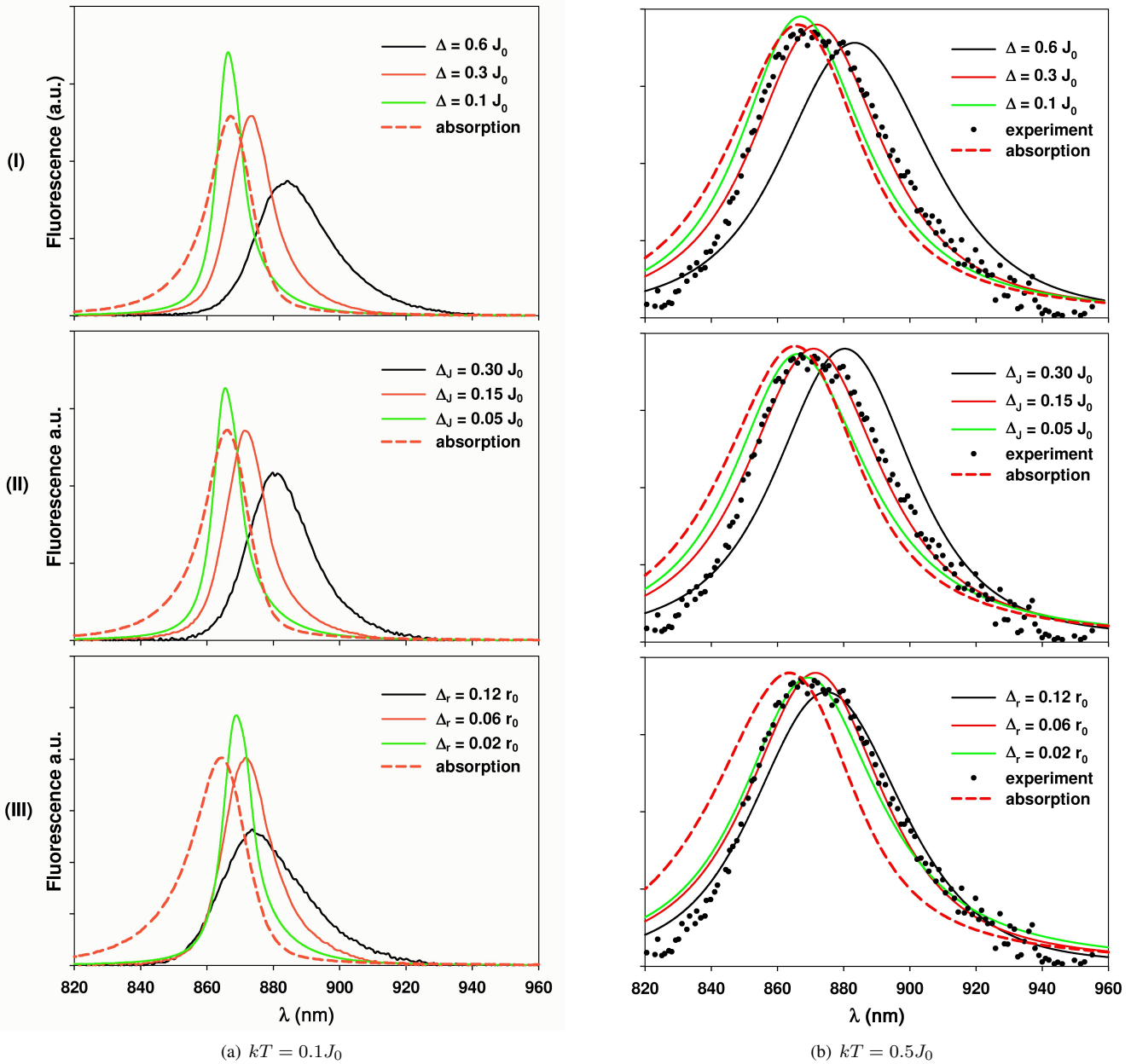


Figure 1. Resulting absorption spectra $OD(\omega)$ and steady-state fluorescence $FL(\omega)$ spectra of LH2 averaged over 2000 realizations of static disorder for three different types of static disorder and for two temperatures. Rows: (I) - Gaussian static disorder in local excitation energies $\delta\varepsilon$, (II) - Gaussian static disorder in nearest neighbour transfer integrals δJ , (III) - Gaussian static disorder in radial positions of molecules δr . Columns: (a) - low temperature $kT = 0.1J_0$, (b) - room temperature $kT = 0.5J_0$. Experimental fluorescence profile averaged in time and over the particles for room temperature [18] (points) is also displayed.

III. COMPUTATIONAL POINT OF VIEW

In the present paper, we are dealing with simulations of absorption spectra and steady state fluorescence spectra for molecular ring, which can model B850 ring from bacterial LH2 complex. Fluorescence $FL(\omega)$ and absorption $OD(\omega)$ spectra have to be simulated for large number of different static disorder realizations. Each realization of static disorder is created by random number generator. Then, so as to have

single ring fluorescence spectrum $FL(\omega)$ and absorption spectrum $OD(\omega)$, it is necessary to put through numerical integrations (see (8), (9)) for each realization of static disorder and finally average these results over all realizations of static disorder. For all calculation, the software package *Mathematica* [26] was used. This package is very convenient not only for symbolic calculations [27], that are needed for expression of all required quantities, but it can be used also for numerical ones [28]. That is why *Mathematica* was

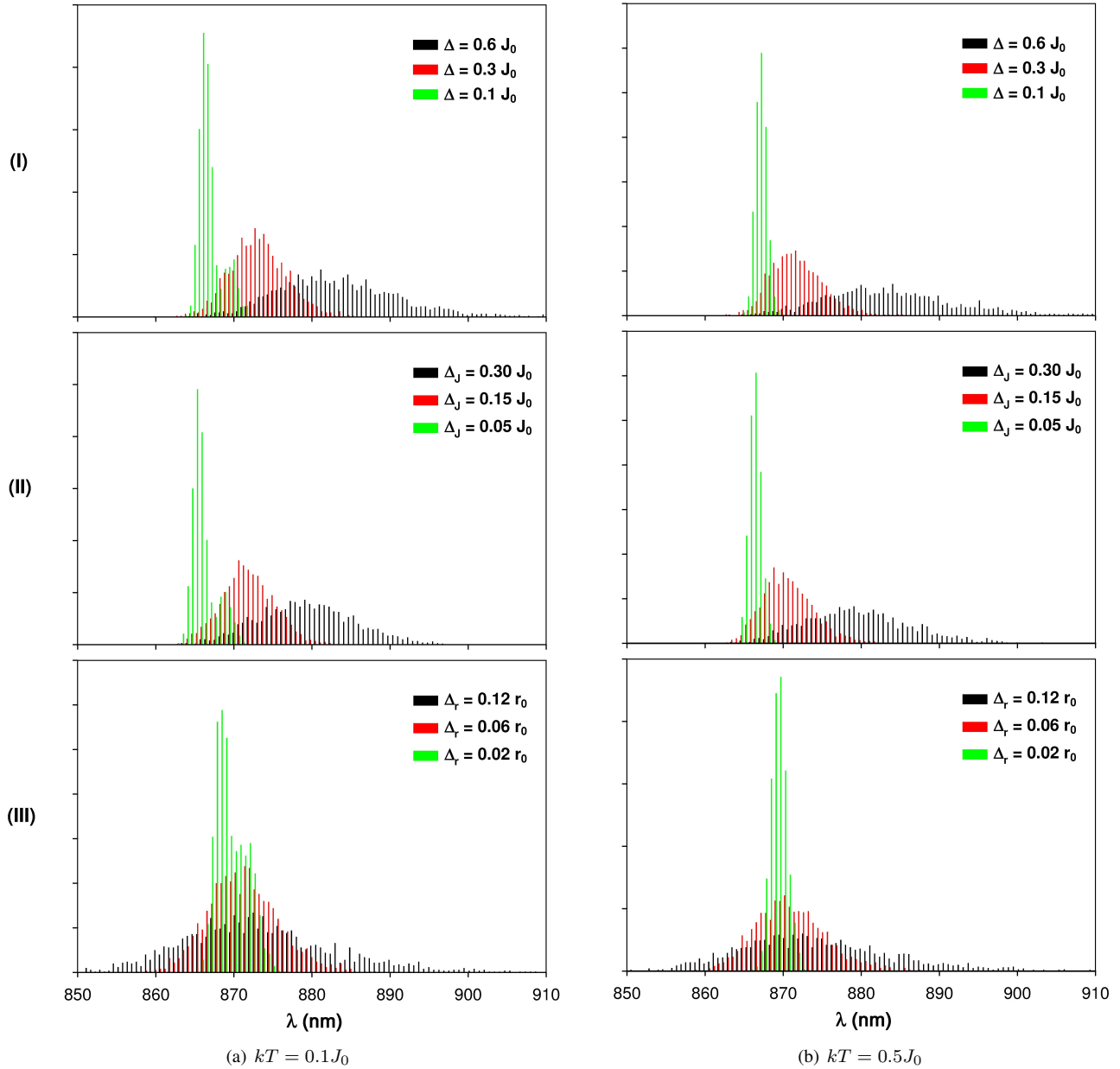


Figure 2. Peak position distributions of calculated steady-state single ring fluorescence spectra $FL(\omega)$ of LH2 for 2000 realizations of static disorder for three different types and three different strengths of static disorder and for two temperatures. Rows: (I) - Gaussian static disorder in local excitation energies $\delta\epsilon$, (II) - Gaussian static disorder in nearest neighbour transfer integrals δJ , (III) - Gaussian static disorder in radial positions of molecules δr . Columns: (a) - low temperature $kT = 0.5J_0$, (b) - room temperature $kT = 0.1J_0$.

used by us as for symbolic calculations as for numerical integrations and also for final averaging of results over all realizations of static disorder.

IV. RESULTS

Three above mentioned types of uncorrelated static disorder have been taken into account in our simulations simultaneously with dynamic disorder in Markovian approximation. Dimensionless energies normalized to the transfer integral $J_{12} = J_0$ have been used. Estimation of J_0 varies in literature between 250 cm^{-1} and 400 cm^{-1} . Contrary to Novoderezhkin et al. [18], different model of spectral density (the model of Kühn and May [12]) has been used. In agreement with our previous results [29] we have used $j_0 = 0.4 J_0$ and $\omega_c = 0.212 J_0$ (see (15)). The strengths of individual types of uncorrelated static disorder have been taken in agreement with [30]. For each type of static disorder, the simulations have been done for three values of the static disorder strength:

- (I) fluctuations in local excitation energies $\delta\varepsilon_n$:
 $\Delta = 0.1, 0.3, 0.6 J_0$,
- (II) fluctuations in transfer integrals δJ_{mn} :
 $\Delta_J = 0.05, 0.15, 0.30 J_0$,
- (III) fluctuations in radial positions of molecules on the ring δr_n :
 $\Delta_r = 0.02, 0.06, 0.12 r_0$, where r_0 is the radius of unperturbed ring.

Resulting steady state fluorescence spectra $FL(\omega)$ and absorption spectra $OD(\omega)$ averaged over 2000 realizations of each static disorder type and strength can be seen in Fig. 1 for low temperature ($kT = 0.1 J_0$, Fig. 1(a)) and for room one ($kT = 0.5 J_0$, Fig. 1(b)).

Comparison of calculated fluorescence spectra with experimental fluorescence profile averaged in time and over the particles at room temperature [18] is also displayed in Fig. 1(b). Simulated fluorescence spectra fitting has been done for middle values of static disorder strength. From this fitting we can determine values of the interpigment interaction energy J_0 and unperturbed transition energy from the ground state ΔE_0 for which the experimental data are best reproduced (the values are given in Section V).

Peak position of single ring fluorescence spectrum depend on the realization of static disorder and also on the temperature. To investigate this effect we calculate peak position distributions of simulated fluorescence spectra for all three above mentioned types of static disorder and for low ($kT = 0.1 J_0$) and room ($kT = 0.5 J_0$) temperature. For each static disorder type we consider three different static disorder strengths (see above). Calculated peak position distributions are shown in Fig. 2.

V. CONCLUSION

Software package *Mathematica* has been found by us very useful for the simulations of molecular ring spectra. For each

above mentioned type of static disorder the experimental fluorescence profile averaged in time and over the particles at room temperature [18] is best reproduced with:

- (I) local excitation energy fluctuations $\delta\varepsilon_n$ (for the standard deviation $\Delta = 0.3 J_0$):
 the interpigment interaction energy $J_0 = 370 \text{ cm}^{-1}$ and unperturbed transition energy from the ground state $\Delta E_0 = 12280 \text{ cm}^{-1}$,
- (II) transfer integral fluctuations δJ_{mn} (for the standard deviation $\Delta_J = 0.15 J_0$):
 $J_0 = 400 \text{ cm}^{-1}$ and $\Delta E_0 = 12350 \text{ cm}^{-1}$,
- (III) fluctuations of radial positions of molecules on the ring δr_n ($\Delta_r = 0.06 r_0$):
 $J_0 = 400 \text{ cm}^{-1}$ and $\Delta E_0 = 12300 \text{ cm}^{-1}$.

The fluorescence spectra shift to higher wavelengths (to lower energies) for increasing static disorder (it can be seen from Fig. 1). This shift is the smallest in case of static disorder in radial positions of molecules (III).

In Fig. 1 the shift of fluorescence spectra peak position to the higher wavelength in comparison with absorption spectra peak position is also visible. This shift is highest (8 nm) for the static disorder type (III).

If the temperature is changed from $kT = 0.5 J_0$ to $0.1 J_0$, the peak position distributions of single ring fluorescence spectra do not alter very much (Fig. 2). At low temperature we can see enlargement of the distribution to the higher wavelengths for all types of static disorder (mainly for small strength of static disorder). At room temperature, this effect is covered by larger widening of single ring spectra caused by dynamic disorder.

ACKNOWLEDGMENT

Support from the Faculty of Science, University of Hradec Králové (project of specific research No. 2116/2011 - P. Heřman and M. Horák) is gratefully acknowledged.

REFERENCES

- [1] G. McDermott, S. M. Prince, A. A. Freer, A. M. Hawthornthwaite, M. Z. Papiz, R. J. Cogdell, and N. W. Isaacs, "Crystal-structure of an integral membrane light-harvesting complex from photosynthetic bacteria," *Nature*, vol. 374, 1995, pp. 517–521.
- [2] M. Z. Papiz, S. M. Prince, T. Howard, R. J. Cogdell, and N. W. Isaacs, "The structure and thermal motion of the B800-850 LH2 complex from *Rps. acidophila* at 2.0 Å over-circle resolution and 100 K: New structural features and functionally relevant motions," *J. Mol. Biol.*, vol. 326, Mar. 2003, pp. 1523–1538, doi:10.1016/S0022-2836(03)00024-X.
- [3] R. Kumble and R. Hochstrasser, "Disorder-induced exciton scattering in the light-harvesting systems of purple bacteria: Influence on the anisotropy of emission and band \rightarrow band transitions," *J. Chem. Phys.*, vol. 109, 1998, pp. 855–865.

- [4] V. Nagarajan, R. G. Alden, J. C. Williams, and W. W. Parson, "Ultrafast exciton relaxation in the B850 antenna complex of *Rhodobacter sphaeroides*," *Proc. Natl. Acad. Sci. USA*, vol. 93, 1996, pp. 13774–13779.
- [5] V. Nagarajan, E. T. Johnson, J. C. Williams, and W. W. Parson, "Femtosecond pump-probe spectroscopy of the B850 antenna complex of *Rhodobacter sphaeroides* at room temperature," *J. Phys. Chem. B*, vol. 103, 1999, pp. 2297–2309.
- [6] V. Nagarajan and W. W. Parson, "Femtosecond fluorescence depletion anisotropy: Application to the B850 antenna complex of *Rhodobacter sphaeroides*," *J. Phys. Chem. B*, vol. 104, 2000, pp. 4010–4013.
- [7] V. Čápek, I. Barvík, and P. Heřman, "Towards proper parametrization in the exciton transfer and relaxation problem: dimer," *Chem. Phys.*, vol. 270, 2001, pp. 141–156.
- [8] P. Heřman and I. Barvík, "Towards proper parametrization in the exciton transfer and relaxation problem. II. Trimer," *Chem. Phys.*, vol. 274, 2001, pp. 199–217.
- [9] P. Heřman, I. Barvík, and M. Urbanec, "Energy relaxation and transfer in excitonic trimer," *J. Lumin.*, vol. 108, 2004, pp. 85–89.
- [10] P. Heřman, U. Kleinekathöfer, I. Barvík, and M. Schreiber, "Exciton scattering in light-harvesting systems of purple bacteria," *J. Lumin.*, vol. 94–95, 2001, pp. 447–450.
- [11] P. Heřman and I. Barvík, "Non-Markovian effects in the anisotropy of emission in the ring antenna subunits of purple bacteria photosynthetic systems," *Czech. J. Phys.*, vol. 53, 2003, pp. 579–605.
- [12] P. Heřman, U. Kleinekathöfer, I. Barvík, and M. Schreiber, "Influence of static and dynamic disorder on the anisotropy of emission in the ring antenna subunits of purple bacteria photosynthetic systems," *Chem. Phys.*, vol. 275, 2002, pp. 1–13.
- [13] P. Heřman and I. Barvík, "Temperature dependence of the anisotropy of fluorescence in ring molecular systems," *J. Lumin.*, vol. 122–123, 2007, pp. 558–561, doi:10.1016/j.jlumin.2006.01.224.
- [14] P. Heřman and I. Barvík, "Coherence effects in ring molecular systems," *Phys. Stat. Sol. C*, vol. 3, No. 10, 2006, 3408–3413, doi:10.1002/pssc.200672119.
- [15] P. Heřman, D. Zapletal, and I. Barvík, "The anisotropy of fluorescence in ring units III: Tangential versus radial dipole arrangement," *J. Lumin.*, vol. 128, 2008, pp. 768–770, doi:10.1016/j.jlumin.2007.12.023.
- [16] P. Heřman, I. Barvík, and D. Zapletal, "Computer simulation of the anisotropy of fluorescence in ring molecular systems: Tangential vs. radial dipole arrangement," *Lecture Notes in Computer Science*, vol. 5101, 2008, pp. 661–670, doi:10.1007/978-3-540-69384-0_71.
- [17] P. Heřman, D. Zapletal, and J. Šlégr, "Comparison of emission spectra of single LH2 complex for different types of disorder," *Physics Procedia*, vol. 13, 2011, pp. 14–17, doi:10.1016/j.phpro.2011.02.004.
- [18] V. I. Novoderezhkin, D. Rutkauskas, and R. van Grondelle, "Dynamics of the emission spectrum of a single LH2 complex: Interplay of slow and fast nuclear motions," *Biophysical Journal*, vol. 90, 2006, pp. 2890–2902, doi:10.1529/biophysj.105.072652.
- [19] W. M. Zhang, T. Meier, V. Chernyak, and S. Mukamel, "Exciton-migration and three-pulse femtosecond optical spectroscopies of photosynthetic antenna complexes," *J. Chem. Phys.*, vol. 108, 1998, pp. 7763–7774.
- [20] S. Mukamel, *Principles of nonlinear optical spectroscopy*. New York: Oxford University Press, 1995.
- [21] A. G. Redfield, "The Theory of Relaxation Processes," *Adv. Magn. Reson.*, vol. 1, 1965, pp. 1–32.
- [22] D. Rutkauskas, V. Novoderezhkin, R. J. Cogdell, and R. van Grondelle, "Fluorescence spectroscopy of conformational changes of single LH2 complexes," *Biophysical Journal*, vol. 88, 2005, pp. 422–435, doi:10.1529/biophysj.104.048629.
- [23] D. Rutkauskas, V. Novoderezhkin, R. J. Cogdell, and R. van Grondelle, "Fluorescence spectral fluctuations of single LH2 complexes from *Rhodospseudomonas acidophila* strain 10050," *Biochemistry*, vol. 43, 2004, pp. 4431–4438, doi:10.1021/bi0497648.
- [24] V. May and O. Kühn, *Charge and Energy Transfer in Molecular Systems*. Berlin: Wiley-WCH, 2000.
- [25] O. Zerlauskienė, G. Trinkunas, A. Gall, B. Robert, V. Urbonienė, and L. Valkunas, "Static and Dynamic Protein Impact on Electronic Properties of Light-Harvesting Complex LH2," *J. Phys. Chem. B*, vol. 112, 2008, pp. 15883–15892, doi:10.1021/jp803439w.
- [26] S. Wolfram, *The Mathematica Book*, 5th ed., Wolfram Media, 2003.
- [27] M. Trott, *The Mathematica GuideBook for Symbolics*. New York: Springer Science+Business Media, Inc., 2006.
- [28] M. Trott, *The Mathematica GuideBook for Numerics*. New York: Springer Science+Business Media, Inc., 2006.
- [29] P. Heřman, D. Zapletal, and I. Barvík, "Computer simulation of the anisotropy of fluorescence in ring molecular systems: Influence of disorder and ellipticity," *Proc. IEEE 12th International Conference on Computational Science and Engineering (CSE '09)*, IEEE Press, vol. 1, 2009, pp. 437–442, doi:10.1109/CSE.2009.88.
- [30] P. Heřman, I. Barvík, and D. Zapletal, "Energetic disorder and exciton states of individual molecular rings," *J. Lumin.*, vol. 119–120, 2006, pp. 496–503, doi:10.1016/j.jlumin.2006.01.042.